Advances in Global MHD Mode Stabilization Research on NSTX

S.A. Sabbagh 1), J.W. Berkery 1), R.E. Bell 2), J.M. Bialek 1), S.P. Gerhardt 2), J.E. Menard 2), R. Betti 3), D.A. Gates 2), B. Hu 3), O.N. Katsuro-Hopkins 1), B.P. LeBlanc 2), F.M. Levinton 4), J. Manickam 2), K. Tritz 5), H. Yuh 4)

1) Department of Applied Physics and Applied Mathematics, Columbia University, New York, NY, USA
2) Princeton Plasma Physics Laboratory, Princeton University, Princeton, NJ, USA
3) Laboratory for Laser Energetics, University of Rochester, Rochester, NY, USA
4) Nova Photonics, Princeton, NJ, USA
5) Johns Hopkins University, Baltimore, MD, USA

e-mail contact of main author: sabbagh@pppl.gov

Abstract. Stabilizing modes that limit plasma beta and reducing their deleterious effects on plasma rotation are key goals for efficient operation of a fusion reactor. Passive stabilization and active control of global kink/ballooning modes and resistive wall modes (RWM) have been demonstrated on NSTX and research now advances to understanding the stabilization physics and reliably maintaining the high beta plasma for confident extrapolation to ITER and CTF. Active n = 1 control experiments with an expanded sensor set, combined with low levels of n = 3 field phased to reduce error fields, reduced resonant field amplification and maintained plasma rotation, exceeded normalized beta = 6, and produced record discharge durations limited by magnet system constraints. Details of RWM active control show the mode being converted to a rotating kink that decays, or saturates leading to tearing modes. Discharges with rotation reduced by n = 3 magnetic braking suffer beta collapse at normalized beta = 4.2 approaching the no-wall limit, while normalized beta greater than 5.5 has been reached in these plasmas with n = 1 active control, in agreement with single-mode RWM theory. Advanced state-space control algorithms proposed for RWM control in ITER theoretically yield significant stabilization improvements. Values of relative phase between the measured n = 1 mode and the applied correction field that experimentally produce stability/instability agree with theory. Experimental mode destabilization occurs over a large range of plasma rotation, challenging the notion of a simple scalar critical rotation speed defining marginal stability. Stability calculations including kinetic modifications to ideal theory are applied to marginally stable experimental equilibria. Plasma rotation and collisionality variations are examined in the calculations. Intermediate rotation levels are less stable, consistent with experimental observations. Trapped ion resonances play a key role in this result. Recent experiments have demonstrated magnetic braking by non-resonant n = 2 fields. The observed rotation damping profile is broader than found for n = 3 fields. Increased ion temperature in the region of maximum braking torque increases the observed rate of rotation damping, consistent with theory.

1. Introduction

Stabilizing large scale magnetohydrodynamic (MHD) modes that limit plasma beta and reducing their deleterious effect on plasma rotation, ω_ϕ, are key goals for efficient operation of a fusion reactor. Demonstrating steady-state high beta conditions in ITER advanced operational scenarios by passive or active means is a key step toward the high beta operation of DEMO. High beta operation is also important to efficiently achieve neutron fluence goals in a nuclear component test facility (CTF) and is required for a demonstration reactor based on the spherical torus (ST) concept. Research on the National Spherical Torus Experiment, NSTX, has demonstrated both passive stabilization [1] and active control [2] of global kink/ballooning modes and resistive wall modes (RWM), accessing high $\beta_t \equiv 2\mu_0 \langle p \rangle / B_0^2$ = 39% and $\beta_N \equiv 10^8 \langle \beta_t \rangle a B_0 / I_p$ = 7.2. Present experiments and analysis now advance toward understanding and optimizing the performance and reliability of active control to maintain the high β_N plasma, understanding global mode stabilization physics, and testing present theories of plasma rotation damping due to non-axisymmetric fields, which are all important for confident extrapolation to future toroidal magnetic fusion systems.

2. Resistive Wall Mode Active Control at Various Plasma Rotation

An expanded set of up to 48 resistive wall mode (RWM) sensors was included in recent active $n = 1$ control experiments to determine optimal sensor configurations and spatial phase, and to increase the reliability of maintaining high β_N greater than the ideal MHD no-wall beta limit, $\beta_N^{no\text{-}wall}$. When this control was combined with low levels of $n = 3$ field phased to reduce error fields, resonant field amplification was reduced and ω_ϕ was maintained, producing record discharge durations in NSTX (up to 1.8s at $I_p = 0.8$ MA) limited by magnet constraints. Without feedback control, high β_N plasmas are more susceptible to RWM instability leading to disruption, even at high levels of ω_ϕ, and to mode locking at reduced rotation. Fig. 1 compares a high β_N discharge using $n = 1$ active mode control with RWM B_p sensor arrays above and below the plasma midplane and $n = 3$ DC error field correction (EFC) to a discharge without active control that is terminated by RWM instability at $\beta_N > \beta_N^{no\text{-}wall}$. In the former case, ω_ϕ is maintained, β_N reaches and exceeds $\beta_N^{no\text{-}wall} = 4$ computed by the DCON stability code and remains above this value with β_N reaching 6 ($\beta_N/\beta_N^{no\text{-}wall} = 1.5$). In the latter case, plasma disruption occurs with ω_ϕ above 8 kHz near the $q = 2$ surface, significantly larger than the critical value for RWM stabilization of 3.8 kHz observed in experiments using $n = 3$ braking for ω_ϕ control. Discharges both with and without reduced rotation can suffer beta collapse at $\beta_N^{no\text{-}wall} = 4.0 - 4.4$, typical for H-mode profiles, while $\beta_N > 5.5$ has been reached at reduced ω_ϕ with $n = 1$ control.

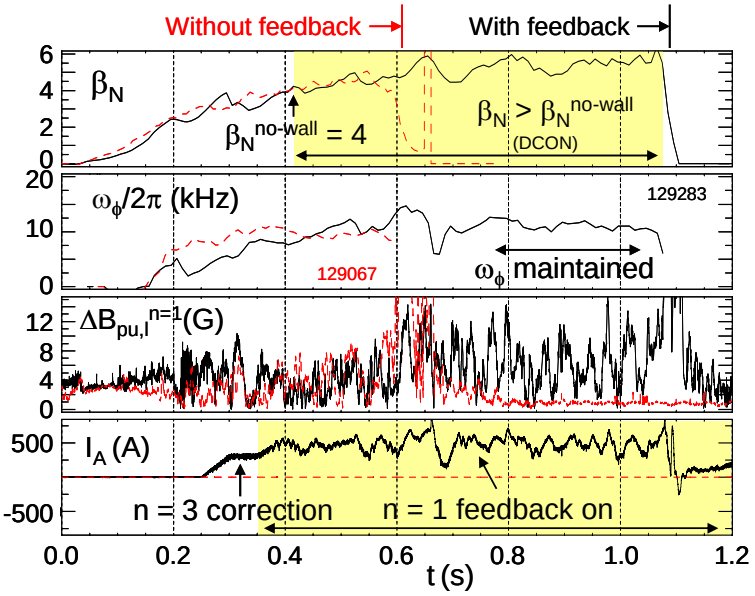

Fig. 1: High β_N discharge using n = 1 active mode control with B_p sensor arrays above/below the plasma midplane and n = 3 DC error field correction (solid line) vs. a discharge without active control (dashed line) that is terminated by an RWM instability at $\beta_N > \beta_N^{no\text{-}wall}$.

Feedback control of $n = 1$ RFA and unstable RWMs was used as a routine tool for the first time in 2008 with more than 200 shots taken in over ten experiments. Two quantifiable measures of success are the probability of reaching long pulse duration and maintenance of high β_N. Restricting the database to standard high performance H-mode operation, high β_N discharges without feedback have a greater susceptibility to RWM-induced disruptions, significantly decreasing the probability of pulse length durations greater than 0.6s (Fig. 2a). With $n = 3$ EFC and $n = 1$ feedback control, I_p flat-top durations of up to 1.6s were achieved. Fig. 2b shows values $<\beta_N>$ and plasma internal inductance $<l_i>$ averaged over the I_p flat-top interval for shots with 0.2s duration (> 60 RWM growth times) and longer. Highest $<\beta_N>$ is maintained with $n = 3$ EFC and $n = 1$ feedback.

Details of $n = 1$ RWM feedback show that control occurs by converting the non-rotating RWM into a global kink which either spins up and stabilizes, or further leads to energy dissipation by tearing modes. This process provides a link between RWM destabilization and tearing mode onset. The conversion from the RWM to a rotating kink occurs on the eddy current decay time of the wall, $\tau_w \sim$ 3-5ms for $n = 1$ modes. In rare cases, which are the most

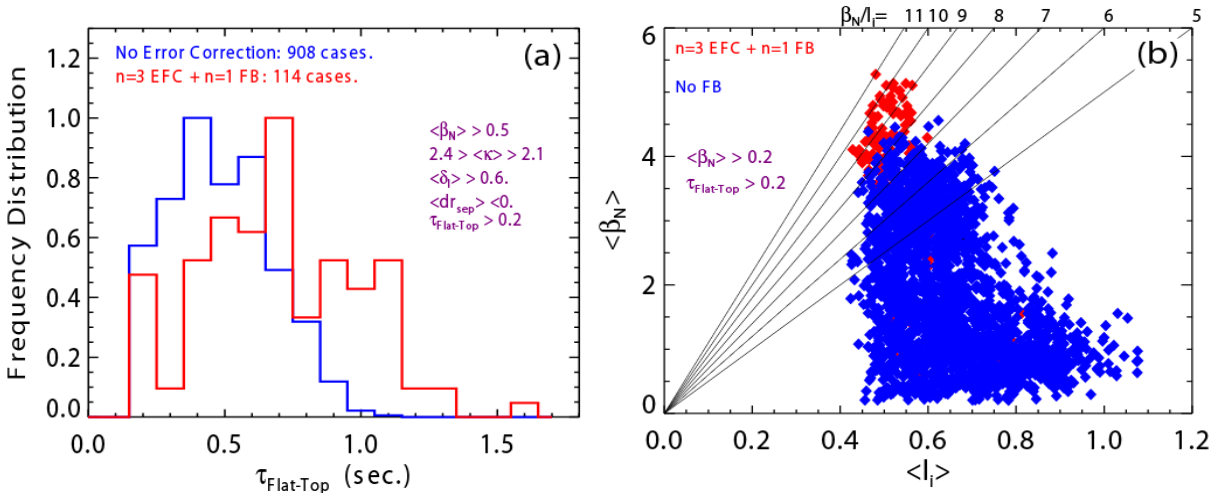

Fig. 2: (a) Frequency distribution of discharge duration for plasmas with standard high performance H-mode plasma shaping with no n=3 EFC and n = 1 feedback control (blue), and with correction and feedback control (red); (b) operational stability space showing level of $<\beta_N>$ for I_p duration > 0.2s without feedback control (blue), and with control (red).

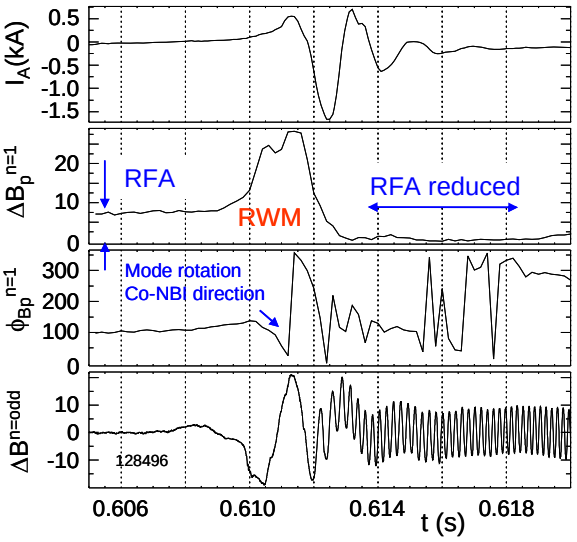

Fig. 3: Detail of RWM evolution and feedback current response under active control.

illustrative, the rotating kink can saturate (Fig. 3). In this case, resonant field amplification observed in the n = 1 amplitude of the RWM poloidal field sensors, $\Delta B_p^{n=1}$, precedes the onset of the RWM. As the mode grows to sufficiently high amplitude, increased drag by the toroidal plasma rotation on the mode causes the RWM to unlock and rotate (shown by the n = 1 RWM phase, $\Phi_{Bp}^{n=1}$). Without feedback control, this signature leads to further RWM growth and disruption [1]. With feedback, the n = 1 control currents (representative current I_A) respond to the mode onset, the RWM unlocks from the wall and accelerates to frequency ~ ω_ϕ, precluding the existence of the RWM which damps in Δt ~ τ_w. The kink displacement is identified by ultrasoft X-ray emission (USXR) and is global (Fig. 4a). USXR emission shows a tearing mode displacement form about 30ms after the saturated kink forms (Fig. 4b).

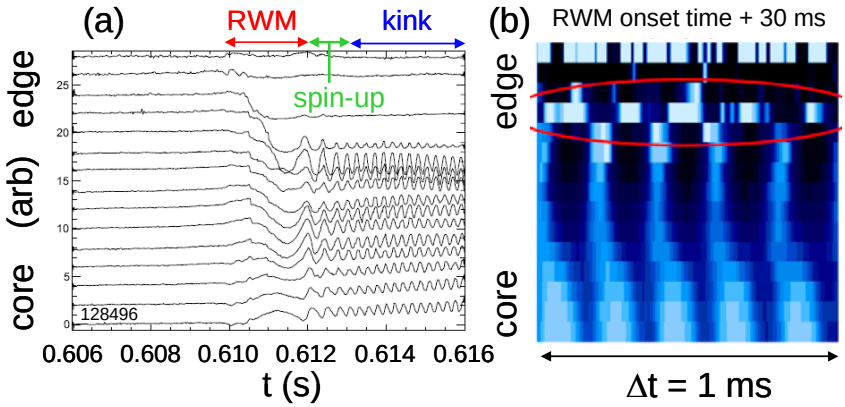

Fig. 4: Ultra-soft X-ray measurement of mode activity during n = 1 feedback control: (a) chord integrated signals spanning from the plasma core to edge show RWM onset, unlock, and spin-up transition to global kink, (b) onset of tearing mode 30 ms after RWM onset, indicated by radial phase inversion of signals (circled).

Specific n = 1 control experiments were run to examine the effect of control system delay on RWM control in ITER-relevant low rotation plasmas. Control system

response was slowed by applying a 75ms smoothing filter to the requested control field currents to preclude response to RWM typical growth times of 3-5ms. With the smoothing filter applied, mode growth led to disruption at $\beta_N > \beta_N^{no\text{-}wall}$ as ω_ϕ was lowered, showing that slow EFC alone is insufficient for stabilization at low ω_ϕ. With no filter, low global rotation, with ω_ϕ near or below DIII-D balanced NBI levels [3], was produced at high $\beta_N = 5.3$.

Experimental active control performance at reduced plasma rotation was reproduced by the VALEN-3D code with an upgraded system model using the actual off-midplane sensor positions and applied control field compensation analogous to that used in the experimental feedback system. Discharges with ω_ϕ reduced by $n = 3$ magnetic braking suffer beta collapse at $\beta_N = 4.2$ while approaching the $n = 1$ ideal MHD beta limit, $\beta_N^{no\text{-}wall}$, as computed by DCON using kinetic/MSE constrained plasma reconstructions (Fig. 5a). In contrast, $\beta_N > 5.5$ has been reached in these plasmas with $n = 1$ active control on. This agrees with single-mode RWM theory using proportional gain. Advanced state-space control algorithms proposed for RWM control in ITER [4] theoretically show potentially large improvements in stabilized $\beta_N < 6.7$. The relative phase, $\Delta\phi_f$, between the measured $n = 1$ mode and the applied correction field theoretically determines if the mode is stabilized or is driven unstable. Values of $\Delta\phi_f$ experimentally producing stability/instability agree with theory (Fig. 5b).

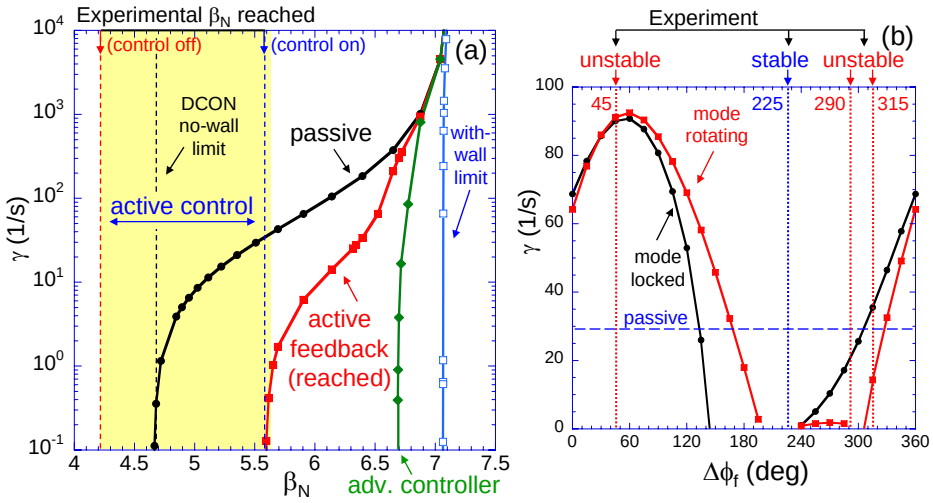

Fig. 5: (a) Experimental β_N reached with $n = 1$ active control with ω_ϕ reduced by $n = 3$ magnetic braking compared to theoretical feedback performance, and computed feedback improvement with an advanced state-space controller; (b) Experimental feedback stability versus feedback phase compared to theory.

3. RWM Passive Stabilization Physics

Passive stabilization of the resistive wall mode by plasma rotation was postulated in seminal theoretical RWM papers [5], however, a comprehensive physics model that unifies experimental RWM stabilization by rotation remains elusive. RWM passive stabilization has been investigated on NSTX, with results summarized in Ref. [6]. While simple RWM models with viscous energy dissipation [7] can qualitatively describe RWM dynamics, simple threshold models of the critical plasma rotation frequency, Ω_{crit}, or disruption due to loss of torque balance by resonant fields [8] do not describe RWM marginal stability in NSTX which is more profound and shown to be at least related to the plasma rotation profile [6]. Recent experiments continue to show this greater complexity. The unstable plasma shown in Fig. 1 becomes unstable at relatively high $\omega_\phi > 8$ kHz near $q = 2$, while plasmas with ω_ϕ lowered by $n = 3$ non-resonant magnetic braking reach marginal stability at $\omega_\phi = 3.8$ kHz. More recently, $n = 3$ magnetic braking has produced marginally stable plasmas that have $\omega_\phi = 0$ at the $q = 2$ surface. A more comprehensive stability model by Hu and Betti including kinetic

modifications to ideal MHD theory [9] has been used evaluate the stability of NSTX plasmas with initial success. Modifications to Ideal Stability by Kinetic effects are computed with the MISK code, including the effect of trapped and circulating ions, trapped electrons, and Alfven damping [10]. The kinetic components of the perturbed pressure lead to a potential energy functional δW_K. The modified RWM growth rate normalized to τ_w is $\gamma\tau_w = -(\delta W_\infty + \delta W_K)/(\delta W_b + \delta W_K)$, where δW_∞ is δW computed with no stabilizing conducting structure and δW_b is computed with a model of the experimental stabilizing conducting structure. The calculation involves an integration over energy of a frequency resonance term (Eq. 5 of Ref. 10). For the trapped ion component,

$$\delta W_K \propto \int \left[\frac{\omega_{*N} + \left(\hat{\varepsilon} - 3/2\right)\omega_{*T} + \omega_E - \omega - i\gamma}{\langle \omega_D \rangle + l\omega_b - i\nu_{eff} + \omega_E - \omega - i\gamma} \right] \hat{\varepsilon}^{\frac{5}{2}} e^{-\hat{\varepsilon}} d\hat{\varepsilon}\,, \qquad (1)$$

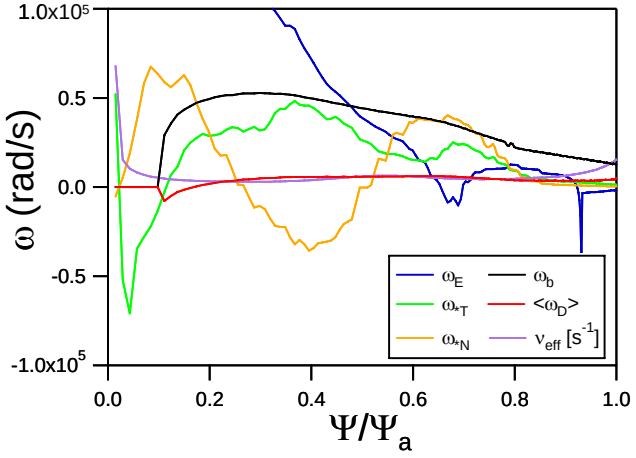

Fig. 6: Frequency profiles for kinetic stabilization of RWM marginally stable plasma 121083 at 0.475s. The collision frequency profile shown is for thermal ions, bounce and diamagnetic frequency profiles are for thermal ions and zero pitch angle.

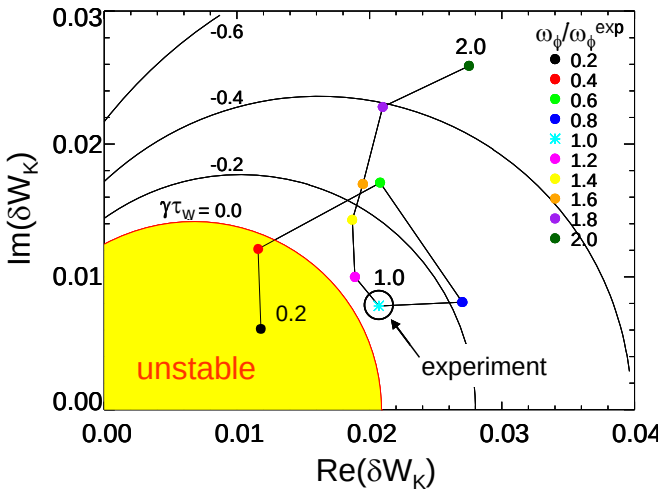

Fig. 7: Effect of plasma rotation on n = 1 RWM stability for plasma 121083 at 0.475s. The markers indicate self-similarly varied ω_ϕ profiles.

where the mode frequency is ω, and $\hat{\varepsilon}$ is the particle energy normalized to the ion temperature. The other six frequencies are compared, as profiles of poloidal flux Ψ, for an RWM marginally stable plasma in Fig. 6 where ω_{*N} and ω_{*T} are the density and temperature gradient components of the ion diamagnetic frequency, ω_E is the $E\times B$ frequency, $\langle\omega_D\rangle$ is the bounce-averaged precession drift frequency, ω_b is the bounce frequency, and $\nu_{\rm eff}$ is the effective collision frequency. Plasma toroidal rotation enters through ion force balance $\omega_E = \omega_\phi - \omega_{*N} - \omega_{*T}$. The resonances in Eq. 1 allow a more complex dependence of stability on the rotation profile. In the plasma shown in Fig. 6, $n = 3$ braking produces a peaked ω_ϕ profile, with sufficiently small $|\omega_\phi| < (\omega_{*N} + \omega_{*T})$ allowing increased δW_K by stabilizing resonance with the trapped ion precession drift in the outer portion of the plasma (roughly $q > 2$). Variation of ω_ϕ from an experimental RWM marginally stable equilibrium reconstruction shows reduced stability at intermediate and low plasma rotation, rather than a simple critical rotation threshold. This is shown by varying the experimental rotation profile ω_ϕ^{exp} and computing $\gamma\tau_w$ for the variations. A stability diagram is produced in which contours of constant $\gamma\tau_w$ are shown on a plot of $Im(\delta W_K)$ vs. $Re(\delta W_K)$ (Fig. 7). The region of $\gamma\tau_w > 0$ which is theoretically unstable to the RWM is highlighted. The rotation profile is varied self-similarly from 0.2 to 2 times the experimental profile. Stability decreases

as plasma rotation decreases from $\omega_\phi/\omega_\phi^{exp}$ = 2.0 to the value 1.0, which represents the measured experimental profile. This point is experimentally observed to be on the verge of instability and is computed to be close to marginal ($\gamma\tau_w$ > -0.1). As ω_ϕ is reduced further, the plasma becomes more stable between 1.0 < $\omega_\phi/\omega_\phi^{exp}$ < 0.6. For low rotation (< 0.4ω_ϕ^{exp}), the plasma is predicted to be unstable. This is consistent with the general NSTX experimental observation that very low global rotation at $\beta_N > \beta_N^{no\text{-}wall}$ is typically unattainable without active n = 1 control. Further physical insight is attained by examining the components of δW_K as rotation is varied. In Fig. 8 the real and imaginary parts of δW_K are broken into the trapped ion, trapped electron, circulating ion and Alfven layer contributions. For $\omega_\phi/\omega_\phi^{exp}$ from 0.2 to 0.6, stability increases as the real and imaginary trapped ion components increase. From 0.6 to 0.8, the real part increases while the imaginary part decreases, leading to the turn in Fig. 7 back towards instability. Finally for $\omega_\phi > \omega_\phi^{exp}$, the trapped ion contributions are nearly constant, but the increase in the circulating ion component leads to increased stability.

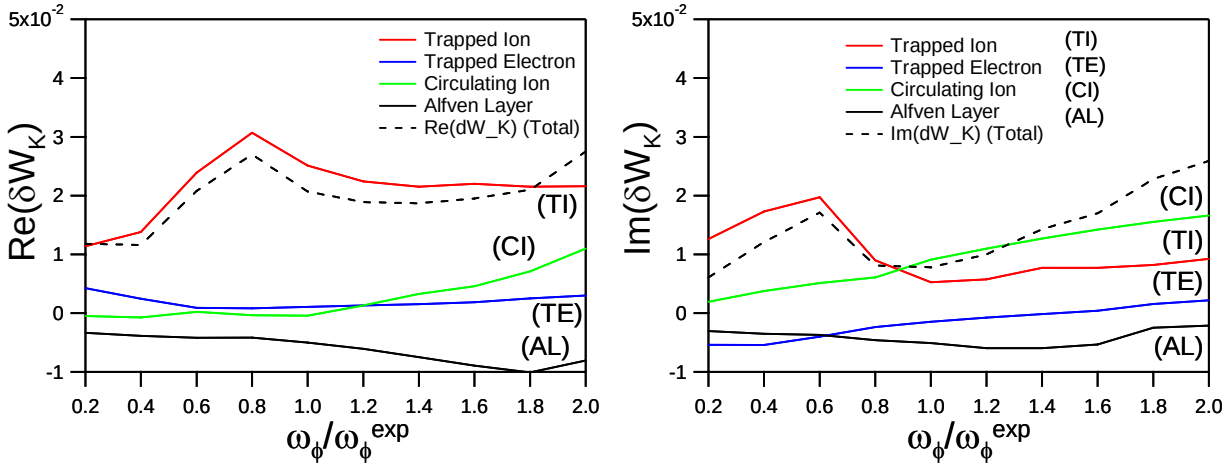

Fig. 8: Components of δW_K for plasma 121083 at 0.475s vs. scaled rotation profile.

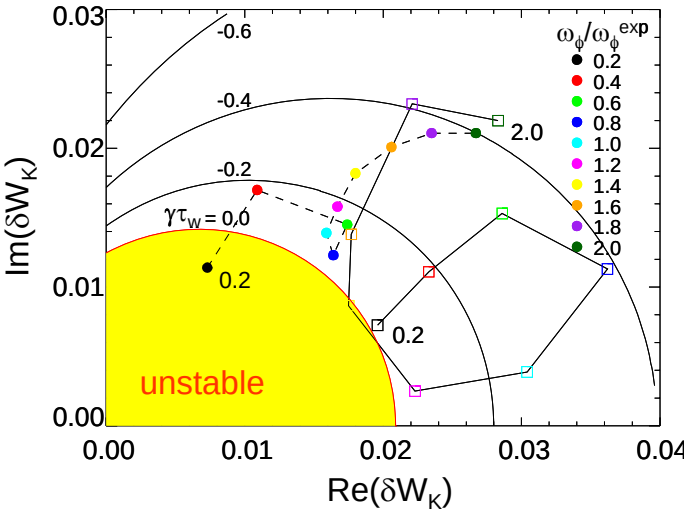

Fig. 9: Effect of plasma collisionality on n = 1 RWM stability for plasma 121083 at 0.475s. Solid circles/dashed line indicates ω_ϕ variation at increased ν, while open squares/solid line show the ω_ϕ variation at decreased ν.

Variation of plasma collisionality, ν, from the experimental equilibrium alters the dependence of stability on rotation. Fig. 9 shows analogous trajectories to Fig. 7, but with electron and ion temperatures halved/doubled while the densities are doubled/halved, producing collisionalities increased/ decreased by a factor of 5.7 while maintaining constant pressure. Increased ν simplifies the dependence of stability on ω_ϕ, making the trajectory appear more like it has a single critical rotation profile for stability. This might be expected, as higher ν decreases the relative importance of the kinetic resonances. Lower ν produces the opposite effect. As ω_ϕ is decreased, there is a broader reversal of $\gamma\tau_w$ from decreasing to increasing stability, marginal stability occurs at higher plasma rotation than in the actual experiment, and the trajectory shows stability at low ω_ϕ.

4. Plasma Rotation Alteration by Even Parity Non-resonant Fields and T_i Dependence

Physics understanding of non-axisymmetric field-induced plasma viscosity is important to ITER, especially if magnetic ELM mitigation techniques will be used, and in CTF if ω_ϕ profile alteration is desired for global mode control. Braking torque due to odd parity applied fields has been observed and quantitatively compared to neoclassical toroidal viscosity (NTV) theory in NSTX [11]. Recent experiments also demonstrate non-resonant braking by an n = 2 field configuration which has a significant n = 4 component (66% of the n = 2 amplitude) as well as n = 8 and 10 components (each 15% of the n = 2 amplitude). The observed rotation damping profile is broader than for n = 3 fields (Fig. 10), which is theoretically expected due to the broader field spectrum and reduced radial falloff of the n = 2 field.

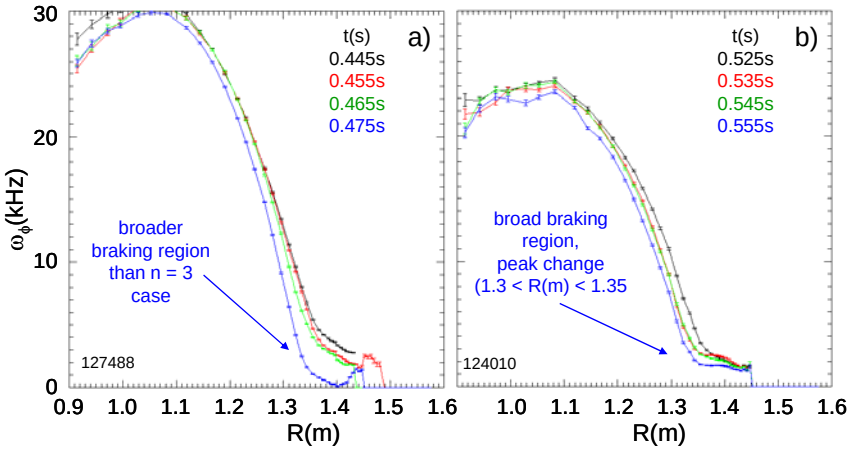

Fig. 10: Comparison of non-resonant magnetic braking by (a) n = 2 field configuration to (b) n = 3 configuration.

A significant aspect of the NTV theory for ITER and a CTF is the strong increase in NTV torque that occurs as the ion collisionality drops below the trapped particle bounce frequency, $\nu_{*i} < 1$. In this ion collisionality regime, the non-ambipolar flux that leads to NTV is decreasingly perturbed by collisions, which increases the NTV torque, causing a strong dependence on ion temperature, $\tau_{NTV} \sim \delta B^2 \varepsilon^{1.5} p_i / \nu_i \sim T_i^{5/2}$ [11]. Recent experiments show that increased T_i increases the plasma rotation damping rate during non-resonant magnetic braking. The experiments utilized lithium evaporation to pre-condition portions of the divertor and plasma facing component carbon tiles [12] to generate a significant increase in T_i in the region of peak n = 2 magnetic braking. Fig. 11 compares two plasmas with equal magnitude of applied n = 2 braking currents, and with/without lithium wall preparation. The plasma with Li preparation shows higher initial T_i (shown in the region of maximum change of ω_ϕ, R = 1.37m) at the start of the magnetic braking pulse, with a ratio of T_i between the two shots of $T_i^{(\mathrm{Li})} / T_i^{(\mathrm{no\ Li})}$ = 1.324. This yields a theoretical increase in τ_{NTV} of a factor of two in the plasma with higher T_i and is consistent with the measured increase in $|d\omega_\phi/dt|$ observed in the plasma. Fig. 12a and Fig. 12b show the plasma rotation profile evolution for these shots. A plasma using Li wall preparation was then run with the braking current reduced by 25% (~ 45% less braking torque) which allowed saturation of the ω_ϕ profile and maintained RWM stability through the braking pulse (Fig. 12c).

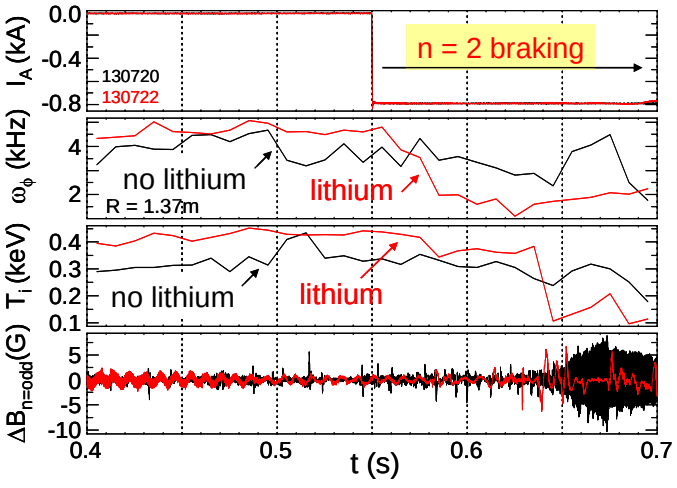

Fig. 11: Comparison of n = 2 magnetic braking in plasmas with varied ion temperature.

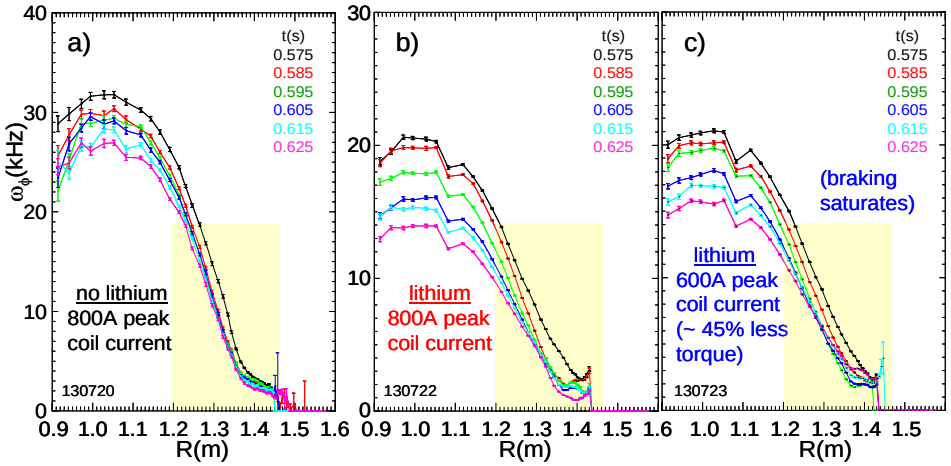

Fig. 12: Evolution of ω_ϕ in discharges slowed by $n = 2$ magnetic braking.

5. Summary and Discussion

With initial passive and active global mode stabilization established on NSTX, research is advancing toward understanding the physics of mode stabilization and to maintaining high beta plasmas with high reliability. RWM instability occurs over a wide range of ω_ϕ, and the combination of $n = 3$ static EFC and $n = 1$ feedback control greatly increases the probability of sustaining high β_N over long pulses, producing record pulse duration in the device, limited by magnet system constraints. RWM dynamics during successful $n = 1$ feedback shows the mode convert to a rotating kink which damps, or saturates typically leading to tearing modes. Fast $n = 1$ feedback control response ~ O(τ_w) is necessary to avoid high β_N plasma disruption at low ω_ϕ. Simple models of a critical rotation threshold for RWM stabilization are too restrictive to explain the observed plasma stability vs. ω_ϕ. A physics model including kinetic modifications to ideal stability shows regions of reduced passive stability at intermediate ω_ϕ as well as low ω_ϕ, which agree with experimental observations. Plasma collisionality alters the range of ω_ϕ displaying reduced stability, which may unify the physics understanding of RWM stability between present STs and tokamaks. Plasma rotation alteration has been demonstrated by magnetic braking using non-resonant $n = 2$ fields. The observed rotation damping profile is broader than that found for $n = 3$ fields. Increasing ion temperature in the region of maximum braking torque increases the observed rate of rotation damping, consistent with the dominant scaling of the non-resonant NTV torque $\tau_{NTV} \sim \delta B^2 \varepsilon^{1.5} p_i / \nu_i \sim T_i^{5/2}$ in the NSTX range of collisionality $\nu_{*i} < 1$. Research at lower ν_i is important to determine at what collisionality the $1/\nu_i$ scaling will saturate and if τ_{NTV} will eventually decrease as ν_i is further reduced.

This research was supported by the U.S. Department of Energy under contracts DE-FG02-99ER54524 and DE-AC02-76CH03073.

[1] S.A. SABBAGH, A.C. SONTAG, J.M. BIALEK, et al., Nucl. Fusion **46** (2006) 635.
[2] S.A. SABBAGH, R.E. BELL, J.E. MENARD, et al., Phys. Rev. Lett. **97** (2006) 045004.
[3] H. REIMERDES, A.M. GAROFALO, G.L. JACKSON, et al., Phys. Rev. Lett. **98** (2007) 055001.
[4] O. KATSURO-HOPKINS, J.M. BIALEK, D.A. MAURER, et. al., Nucl. Fusion **47** (2007) 1157.
[5] A. BONDESON, and D.J. WARD, Phys. Rev. Lett. **72** (1994) 2709.
[6] A.C. SONTAG, S.A. SABBAGH, W. ZHU, et al., Nucl. Fusion **47** (2007) 1005.
[7] R. FITZPATRICK. Phys. Plasmas **9** (2002) 3459.
[8] A. GAROFALO, G.L. JACKSON, R.J. LAHAYE, et al., Nucl. Fusion **47** (2007) 1121.
[9] B. HU and R. BETTI, Phys. Rev. Lett., **93** (2004) 105002.
[10] B. HU, R. BETTI, J. MANICKAM, Phys. Plasmas **12** (2005) 057301.
[11] W. ZHU, S.A. SABBAGH, R.E. BELL, et al., Phys. Rev. Lett. **96** (2006) 225002.
[12] D.K. MANSFIELD, H.W KUGEL, R. MAINGI, et al. "Transition to ELM-free improved H-mode by lithium deposition on NSTX graphite divertor surfaces", in proceedings of the 18th PSI meeting, Toledo, Spain May 26-30, 2008, paper O-28; accepted for publication in Jour. Nucl. Mater.